

To appear in ApJ.

GU Boo: A New $0.6 M_{\odot}$ Detached Eclipsing Binary

Mercedes López-Morales^{1,2}

*Carnegie Institution of Washington, Department of Terrestrial Magnetism, 5241 Broad
Branch Rd. NW, Washington D.C., 20015, USA*

mercedes@dtm.ciw.edu

and

Ignasi Ribas

*Institut d'Estudis Espacials de Catalunya/CSIC, Campus UAB, Facultat de Ciències,
Torre C5 - parell - 2a planta, 08193 Bellaterra, Spain*

iribas@ieec.uab.es

ABSTRACT

We have found a new low-mass, double-lined, detached eclipsing binary, GU Boo, among a sample of new variables from the ROTSE-I database. The binary has an orbital period of 0.488728 ± 0.000002 days, and estimated apparent magnitudes $V_{\text{rotse}} \simeq 13.7$ and $I \simeq 11.8$. Our analysis of the light and radial velocity curves of the system yields individual masses and radii of $M_1 = 0.610 \pm 0.007 M_{\odot}$, $M_2 = 0.599 \pm 0.006 M_{\odot}$, $R_1 = 0.623 \pm 0.016 R_{\odot}$, $R_2 = 0.620 \pm 0.020 R_{\odot}$. The stars in GU Boo are therefore very similar to the components of the eclipsing binary YY Gem. For this study we have adopted a mean effective temperature for the binary of $T_{\text{eff}} = 3870 \pm 130$ K. Based on its space velocities we suggest that GU Boo is a main sequence binary, possibly with an age of several Gyr. The metallicity of the binary is not well constrained at this point but we speculate that it should not be very different from solar. We have compared the physical parameters of GU Boo with current low-mass stellar models, where we accounted for uncertainties in age and metallicity by considering a wide range of values for

¹Carolina Royster Society Fellow 2003-2004.

²Visiting Astronomer at the Southeastern Association for Research in Astronomy (SARA) Observatory.

those parameters. Our comparisons reveal that all the models underestimate the radii of the components of GU Boo by at least 10–15%. This result is in agreement with the recent studies of YY Gem and CU Cnc.

Subject headings: binaries: eclipsing — binaries: spectroscopic — stars: fundamental parameters — stars: late-type — stars: individual (GU Boo)

1. Introduction

At least 70% of the stars in the Galaxy are low-mass objects, meaning that they have masses below $1 M_{\odot}$. In spite of their large number, our understanding of the physics at work in low-mass stars is still at a basic stage. Much effort has been put in recent years into the development of reliable models for low-mass stars (see reviews by Chabrier & Baraffe 2000 and Allard et al. 1997). As a result of those efforts, the state-of-the-art models now reproduce fairly well some of the parameters of low-mass stars, such as the observed mass- M_V and mass-luminosity relations (e.g., Delfosse et al. 2000). However, the same models still fail to reproduce other fundamental parameters, such as the stellar effective temperature (T_{eff}) scale and, most notably, the mass-radius relation (Torres & Ribas 2002; Ribas 2003).

As recent papers on low-mass binaries have repeatedly stated, the main problem encountered when trying to test the models of low-mass stars is the scarcity of accurate empirical measurements of fundamental parameters of those objects, in particular, accurate values for both their masses and radii. Accurate masses and radii (with errors $\sim 1\text{--}2\%$) can only be derived from double-lined, detached, eclipsing binaries (DDEBs), but until now only three DDEBs reaching such high accuracies in their properties had been found and analyzed in detail. Those binaries are YY Gem (Lacy 1977; Torres & Ribas 2002), CU Cnc (Delfosse et al. 1999; Ribas 2003), and CM Dra (Leung & Scheneider 1978; Metcalfe et al. 1996). Note that new masses and radii have been recently derived for two other binaries, BW3 V38 (Maceroni & Montalbán 2004) and TrES-Her0-07621 (Creevey et al. 2005). However, the current measurement uncertainties are too large to constrain the models.

We present in this work a new DDEB, GU Boo [$\alpha(\text{J2000}) = 15:21:55.16$, $\delta(\text{J2000}) = +33:56:04.1$], composed of two similar stars of about $0.6 M_{\odot}$ with apparent magnitudes $V_{\text{rotse}} \simeq 13.7$ and $I \simeq 11.8$, and an orbital period close to 0.5 days. The two new masses and radii from GU Boo increase by 40 percent¹ the current number of accurate measurements of those

¹In the analysis of Torres & Ribas (2002), the two stars in YY Gem were assumed to be identical. Therefore they count only as one object for statistical purposes.

parameters for stars below $1 M_{\odot}$, providing two new key empirical points to test the models.

GU Boo was first reported as a variable object by Diethelm (2001), who listed it as a new *eclipsing Algol system* found among light curves from phase I of the Robotic Optical Transient Search Experiment (ROTSE-I; Akerlof et al. 2000). There is no reference to this binary in the literature previous to Diethelm’s identification, and it only appears in the Guide Star Catalog (Lasker et al. 1996) as star GSC 02566-00776, and as ROTSE1J152155.16+335604.1 in the ROTSE-I database (Akerlof et al. 2000). The variable star name V^* GU Boo was assigned to this system by Kazarovets et al. (2003), after Diethelm’s identification.

We identified the system as a low-mass binary based on the short orbital period reported by Diethelm and on the estimated width of the eclipses from the ROTSE preliminary light curve. Using the orbital period, the width of the eclipses, and Kepler’s Third Law we estimated a preliminary total mass for the system of $M_1 + M_2 \leq 1.3 M_{\odot}$. This way of estimating the total mass of binaries is only valid for systems with $q \simeq 1.0$, and close to edge-on ($i \simeq 90^{\circ}$) orbital inclinations. In any other case, the estimated $M_1 + M_2$ represents only a lower limit to the actual total mass of the binary. We subsequently obtained complete R- and I-band light curves and radial velocity curves of the binary to derive its masses and radii with enough accuracy to test the models. In the following sections of this paper we report the physical properties of GU Boo that have resulted from our detailed analysis of the light and radial velocity curves, and we compare those properties to the current models.

2. Mean Effective Temperature

The temperature scale of the lower main sequence is yet weakly established, the reason being the lack of an statistically significant sample of low-mass stars with reliable bolometric fluxes, distances, and radii. The increasing number of eclipsing binaries and nearby stars resolved interferometrically should soon put a solution to this long-standing problem. In the mean time, to determine the temperature of M-type stars we need to rely on the use of various empirical and model-dependent calibrations, which are usually built upon one or more photometric indices.

We have carried out mean temperature estimations of GU Boo using several available calibrations. Empirical and model-dependent calibrations have been used separately to have a better measure of possible systematic errors. In Table 1 we summarize the magnitudes of GU Boo collected from the literature, and used to derived the color indexes listed in Table 2. The first two columns of Table 2 summarize the calibrations and color indexes that we used to estimate the mean T_{eff} of GU Boo. The values of the effective temperatures resulting

from each calibration are listed in column 3.

The average temperature of GU Boo from the empirical calculations is 3900 ± 120 K, while the one obtained from the model-dependent calibrations is 3830 ± 135 K. In all cases the temperature resulting from the (V-I) index is generally some 200 K lower than that obtained from the (V-K) index. This may be indicative of some inaccuracies in the photometry. The relatively large error bar in the resulting temperatures is a reflex of such inconsistencies.

The average effective temperatures derived from each set of calibrations (empirical and model-dependent) agree within the estimated errors. Given this good agreement, we decided to take as the mean temperature of GU Boo the average of both results. The mean effective temperature of GU Boo adopted in our study is therefore 3870 ± 130 K. Note that the mean temperature of GU Boo is very close to the temperature of YY Gem determined by Torres & Ribas (2002). This is not surprising since the optical/IR colors of the two systems are quite similar.

As a caveat to this temperature estimation, note that we have used color indexes collected from the literature, for which we lack information about the epochs of each observation. Some of the magnitudes (colors) could have been collected during eclipse epochs, and therefore the temperatures derived from those colors would deviate from the real value of T_{eff} . The colors will be also affected if the magnitudes were measured at epochs when the binary was undergoing different levels of activity. Note also that the V magnitude of GU Boo is an approximate calibration (V_{rotse}) from the ROTSE-I database (Akerlof et al. 2000)². BVRI and JHK calibrated photometry of GU Boo is currently underway at specific out-of-eclipse orbital phases, and we expect to derive from this photometry more accurate colors that will provide a more accurate estimation of the mean T_{eff} of GU Boo.

3. Radial Velocity Curve Observations and Analysis

3.1. Observations

We collected spectra covering the entire orbital phase space of GU Boo in two nights, May 9-10 and May 18-19, 2003, with the echelle spectrograph at the 4-m Mayall telescope at Kitt Peak. The spectra from the first night covered a wavelength range of 310–860 nm

²The ROTSE-I instrumental magnitudes m_{rotse} have been calibrated to set their zero point onto a V-band equivalent scale. The recalibration procedure is explained in detail in Akerlof et al. (2000).

per frame, with an average resolving power of $\lambda/\Delta\lambda = 18,750$ at 6000 \AA . The configuration of the spectrograph on the second night was slightly different (different cross-disperser) to accommodate the needs of a parallel observing program. The resolving power of the new configuration was the same as in night 1, but with a larger wavelength coverage, 310–1010 nm. We collected a total of 103 spectra of GU Boo in those two nights, with average S/N between 6.5 and 9.0 (exposure times between 120 and 180 seconds). We also collected spectra of the M dwarfs GJ 410 and GJ 361 with each spectrograph configuration, to use them as templates in the subsequent analysis of the radial velocities of GU Boo. The average S/N of the spectra of those templates are, respectively, 82.5 and 67.0.

3.2. Analysis

Radial velocities were extracted from the spectra of GU Boo using the implementation of the two-dimensional cross-correlation algorithm TODCOR (Zucker & Mazeh 1994) by G. Torres and D. Latham at the Harvard-Smithsonian Center for Astrophysics (CfA). The analysis of GU Boo with TODCOR was done following a procedure analogous to the one described in detail by Torres & Ribas (2002) in their analysis of YY Gem.

We used the spectra of the M dwarfs GJ 410 (M0 V) and GJ 361 (M1.5 V) as trial templates instead of the using synthetic spectra, the common procedure for more massive stars. The reasoning behind this decision is that the synthetic spectra computed using stellar atmosphere models reproduce well the spectral features observed in real stars down to $0.60\text{--}0.65 M_{\odot}$ ($T_{\text{eff}} \leq 4000 \text{ K}$). However, for stars below $\simeq 0.6 M_{\odot}$, as is the case of GU Boo, the synthetic spectra generated by the models deviate significantly from the ones observed. This is because the current models do not include all the sources of molecular opacity that become relevant below 4000 K, as is for example the case of the H_2O molecule. To avoid the incompleteness of the models we used instead spectra of real stars of spectral type similar to the components of the binary.

Optimal results with TODCOR are attained when the rotational broadening of the templates matches the broadening of the components of the binary. We artificially broadened the spectra of the templates by different amounts of $v \sin i$, and ran extensive tests to determine the combination of templates and rotational broadenings that best matched the spectra of GU Boo. The results of those tests using GJ 410 as template for both stars are shown in Figure 1. Similar tests using GJ 361 for each star and GJ 410 and GJ 361 for either the primary or the secondary gave always lower correlation coefficients than the tests using GJ 410 for the two stars. The highest value of the correlation coefficient in TODCOR indicates the best match between the observed spectra and the combination of broadened templates.

In this case, as illustrated in the figure, the highest value of the cross-correlation coefficient occurred when we used GJ 410 as template for both stars, broadened by 65 km s^{-1} for the primary and 58 km s^{-1} for the secondary.

The S/N in each order of the echelle spectra degrades towards the edges because of the blaze function of the spectrograph. When this effect is combined with the already low S/N of the data, the information in those edges turns out to be too poor even for a technique as sensitive as TODCOR. We removed the very-low S/N parts of the spectra by trimming in each aperture the edge portions with $S/N \leq 3.5$. We also discarded all the apertures that had S/N below that threshold, or that contained prominent non-stellar absorption bands or emission lines. The radial velocity curves were derived running TODCOR separately for each aperture and then computing an average radial velocity per frame for each star. The resulting radial velocities correspond to the average of all the apertures in each frame, after eliminating the values that deviate more than 2σ from the mean. The typical standard deviation of the average velocities is 10 km s^{-1} or better.

We also checked for possible systematic effects in the individual velocities derived from TODCOR by performing numerical simulations. We generated 103 artificial binary spectra by combining templates of GJ410 with different velocity shifts. The velocity shifts were computed from the best available orbital solution of GU Boo and the times when the real observations of the binary were taken. We then ran TODCOR substituting the real observations by the synthetic spectra to measure any systematics. No clear systematic trend was noticed, and the observed differences between the input and output velocity shifts were of the same order as the average velocity dispersion per frame. Finally, we found that the changes in the orbital solution of the radial velocity curves after correcting for the errors suggested by the simulations were insignificant, therefore we did not correct for these residuals in the computation of the final spectroscopic orbital solution of GU Boo.

The final radial velocity curves are shown in Figure 2. The filled circles in that curve correspond to the radial velocity of the primary, the open circles to the radial velocity of the secondary, and the solid and dashed lines show the best orbital solution fits. Table 3 summarizes the parameters of the spectroscopic orbital solution derived from those curves. In that solution we adopted the orbital period $P(\text{days})$ and initial epoch $T_0(\text{HJD})$ derived in §4.2. We left the eccentricity of the orbit as a free parameter during the preliminary stages of the computation of the orbital solution and then ran several tests using different initial values of that eccentricity. Those tests resulted on an average orbital eccentricity of $e=0.0001 \pm 0.0038$, which suggests a circular orbit for the binary. Based on this result, the eccentricity of the orbit of GU Boo was set to zero in the analysis.

Systematic errors in the radial velocities could be caused by the spots on the surface

of the stars. We evaluated this effect using the spot scenario adopted in §4.3 and found systematic deviations in the velocity semi-amplitudes of the order of 0.5 km s^{-1} . Note from the values of K_1 and K_2 in Table 3 that 0.5 km s^{-1} nearly corresponds to the 1σ errors reported for those parameters. We could not, however, apply the corrections to the radial velocities because the photometric and spectroscopic observations were not contemporaneous and possibly had different spot configurations. Thus, we caution that systematic errors in K_1 and K_2 of the same order of the random errors could be present.

The radial velocity data in Figure 2 is available in electronic form from the ApJ website. The contents of the electronic table are illustrated in Table 4. The velocities in that table have been corrected to the heliocentric reference system by adopting a peculiar velocity of -13.9 km s^{-1} for the template of GJ 410 (Gliese 1991).

In addition to extracting the radial velocity semi-amplitudes of the stars in the binary, the cross-correlation algorithm TODCOR (Zucker & Mazeh 1994) also computes their luminosity ratio, independently from the light curve analysis. The luminosity ratio $\alpha = L_2/L_1$ is implemented in TODCOR as an additional parameter to account for the relative intensity of the spectrum of each star. The value of α can be fixed by the user or left free, letting the algorithm compute it as the value that maximizes the correlation parameter in TODCOR for a set of templates. We estimated the luminosity ratio of GU Boo as a function of wavelength by leaving α as a free parameter, and fixing the rest of the parameters in TODCOR to the values used to derive the spectroscopic orbital solution. The results are presented in Figure 3. The relatively large dispersion of the results is a consequence of the low S/N of the data. We applied a linear fit, represented by the continuous line in the figure, which yields an average value of the luminosity ratio of $L_2/L_1 \simeq 0.84 \pm 0.04$ at 6200 \AA . We believe that the slight slope of the fit is real, and that it is caused by the difference in temperature of the two components.

4. Light Curve Observations and Analysis

4.1. Observations

We obtained complete R- and I-band light curves of GU Boo using standard CCD differential photometry techniques. The data were collected over 7 nights between March 24 and May 6 2003, at the Southeastern Association for Research in Astronomy (SARA) 0.9-m telescope at Kitt Peak. The average photometric accuracy of individual measurements is 0.003 mag in R and 0.004 mag in I, respectively.

The SARA telescope was equipped with an Ap7 512×512 CCD that provided a field-

of-view of $6' \times 6'$. GU Boo is a relatively faint target ($V_{\text{rotse}} \simeq 13.7$), with not many other objects of similar spectral type or brightness nearby. By placing GU Boo close to one of the corners of the CCD, we managed to strategically locate the binary on the chip together with two other stars of similar apparent magnitude. As comparison star we selected GSC 02566-00631, located $2'59$ away from the target. The check star was chosen to be GSC 02566-00935, at about $4'53$ from GU Boo, and $1'94$ from the comparison star. Both stars passed respective tests for intrinsic photometric variability and proved to be stable during the time span of our observations.

We collected a total of 492 measurements in the R band and 947 in the I band with exposure times of 120 and 60 seconds, respectively. The observations covered the entire orbit of the binary in each filter. The data were analyzed using standard aperture photometry packages in IRAF, with no differential extinction effects taken into account given the relative small separation between the target and the comparison and check stars.

The R and I light curves of GU Boo that resulted from including all the data above presented significant scatter in brightness (of up to 0.1 mag) over all orbital phases. The apparent time scale of those brightness variations is of the order of days to weeks, and we attribute them to migration of spots on the surface of the stars. However, the photometry is fairly stable within a given night, with most of the scatter appearing at orbital phases when observations made several days or weeks apart overlap. The photometric dispersion of the light curves was substantially reduced by only using the data from nights that (i) when combined cover most parts of the orbital phases of the system, and (ii) were collected close enough in time for the effect of spot migration to be minimal, so the spots can be satisfactorily modeled.

4.2. Orbital Period and Ephemeris

The first to provide an orbital period and zero epoch for GU Boo was Diethelm (2001). Diethelm, using the preliminary light curve from ROTSE-I (Akerlof et al. 2000), measured an orbital period of $P = 0.488722 \pm 0.000002$ days, and established the initial epoch $T_0(\text{HJD}) = 2451222.8497 \pm 0.0012$ for the occurrence of the primary eclipses of the system. However, given that the quality of the ROTSE-I light curve used by Diethelm is rather poor, we decided to check his results using the ephemeris from our new light curves. Our data covers seven different eclipse epochs, including four primary and three secondary minima. Accurate times for those minima were computed by applying 6th order polynomial fits to the light curve data during the eclipses. The values that we obtained are listed on the third column of Table 5. A linear least squares fit to the four primary minima in that table yields

an orbital period of $P = 0.488728 \pm 0.000002$ days, which is in acceptable agreement with the value found by Diethelm. As new reference epoch we have adopted the first time of minimum of the primary eclipse in our data, i.e. $T_0(\text{HJD}) = 2452723.9811 \pm 0.0003$. The re-derived ephemeris equation of the binary is therefore:

$$T(\text{Min I}) = \text{HJD}2452723.9811(3) + 0.488728(2) \cdot E \quad (1)$$

The (O-C) residuals for each time of minimum, i.e. the difference between the observed times of minima and the ones predicted by the ephemeris equation above, are listed in the last column of Table 5. The average residuals are 0.00000 ± 0.00037 days and 0.00030 ± 0.00029 days for the primary and secondary minima, respectively. Using the new orbital period derived above we find an average phase difference between primary and secondary eclipse minima of $\Delta\phi = 0.49981 \pm 0.00033$, which suggests a circular orbit.

4.3. Analysis

The final light curves used in our analysis contain 365 observations in R and 622 in I and are shown in Figure 4. Table 6 lists the dates when the data in Figure 4 were collected, the range of orbital phases covered by those observations, and the number of data points per phase interval. A few sample R-band light curve measurements are listed in Table 7. The full R and I-band photometry tables are available in electronic form from the ApJ website.

Both R and I light curves were fitted simultaneously using the May 2003 version of the Wilson-Devinney program (Wilson & Devinney 1971, May 2003 revision; WD2003 hereafter). We fixed beforehand as many of the free parameters in WD2003 as possible to reduce computing time and convergence problems. The values assigned to those parameters are based on information from external sources or from preliminary fits to the light curves (see column 5 in Table 8).

We assigned to GU Boo a detached binary configuration after ruling out the contact binary scenario, since the estimated ratio of the stellar radii to the Roche lobe radius is $r_*/r_{\text{rl}} \simeq 0.58$. For completeness, we also included reflection and proximity effects in the fits, although there is no clear evidence for such effects in the light curves.

Wilson-Devinney takes into account the effect of limb darkening, gravity brightening, and bolometric albedo when computing the fluxes of the stars. To model the limb darkening we chose a square-root law like the one proposed by Díaz-Cordovés & Giménez (1992). The first and second order limb darkening coefficients were interpolated from tables computed from the Phoenix atmosphere models (e.g., Allard & Hauschildt 1995). Since the tempera-

tures may change during the fitting process, the limb darkening coefficients were recomputed for each iteration of WD2003 whenever necessary. The gravity brightening coefficients were set to 0.2 for both stars, based on the values proposed by Claret (2000). Finally we set the bolometric albedo coefficients to 0.5, which is the standard value for stars with fully convective envelopes, as is the case of the components of GU Boo.

We used the orbital solution of the radial velocity curves (§3.2) to set the mass ratio of the binary to $q = M_2/M_1 = 0.9832$, and the eccentricity of its orbit to zero (although we ran some initial fits to the light curves to further confirm the circularity of the orbit). We also conducted a number of tests to evaluate the presence of any third light (L_3) in the light curves. Those tests yielded null results. The orbital period and the initial epoch of GU Boo were adopted as $P = 0.488728$ days and $T_0(\text{HJD}) = 2452723.9811$, respectively, using the values of the ephemeris derived above. We also assumed that the stars are rotating synchronously. This assumption later proved to be consistent with the radii and orbital inclination resulting from the fit and with the rotational velocities of the stars estimated from the rotational broadening of the spectra (§3.2).

After setting all the parameters above we ran WD2003 iteratively to find the best solution for the remaining light curve parameters. The parameters left free were a phase shift ϕ , the orbital inclination of the binary i , the temperature of the secondary T_2 , the surface potential of each star, Ω_1 and Ω_2 , the luminosity of the primary L_1 , and the spot parameters. We assigned the same statistical weight to each individual observation within a light curve. As relative weight between light curves we used the mean standard deviation of the measurements in each curve (0.003 mag in R and 0.004 mag in I, respectively). The WD2003 iterations were run automatically and a solution was defined as the set of parameter values for which the differential corrections suggested by the code were smaller than the statistical errors for three consecutive iterations (e.g., Kallrath & Milone 1999). We ran a number of fits with different starting values to explore the full parameter space and to avoid missing the global minimum for a local minimum.

The initial tests indicated that the convergence on most of the free parameters was very fast. However, we soon realized that the optimization of spot properties would highly complicate the analysis. Widely differing spot configurations can lead to light curve fits of almost identical quality ³. The intrinsic properties of the binary components are seldom noticeably affected by the adopted spot parameters and, quite often, reaching a good fit

³The ambiguity of photometric solutions for spotted binaries is a well-known problem and was one of the reasons to develop Doppler imaging techniques (see, e.g., Bell et al. 1990; Maceroni & Van’t Veer 1993; van Hamme et al. 2001).

to the out-of-eclipse variations can be regarded as an aesthetic exercise. GU Boo turned out to be somewhat of an exception to this general behavior. We found that different spot parameters do have a rather sizeable effect on the physical properties of the components. Thus, careful modeling of the stellar spots on the components of GU Boo is indeed a critical issue.

We explored a wide range of spot scenarios in an attempt to reproduce the out-of-eclipse brightness variations of the light curves. We also carried out tests to evaluate the sensitivity of the light curve to variations of each spot parameter (latitude, longitude, angular radius, temperature relative to the photosphere, i.e. temperature factor). The fits turned out to be marginally better when the spots have central latitudes in the range $30 - 45^\circ$. Our result can be compared with the theoretical calculations of Granzer et al. (2000) who found that the most likely latitude location for spots on the surface of $0.6 M_\odot$ main sequence stars is $\sim 45^\circ$. Our tests also revealed that the fitting procedure was extremely unstable when more than two spot parameters were left to vary. To decouple this correlation we ran WD2003 using the so-called Method of Multiple Subsets (MMS). MMS allows parameters to be fitted on separate subsets, forcing strongly correlated parameters to converge independently.

We ran series of fits for different number of spots, temperature factors, longitudes, and angular sizes. Our tests started with one dark spot (i.e. temperature factor smaller than 1) on either component. The fit in this case was better than the solution with no spot but the residuals still showed strong systematic deviations. Thus, we tried a series of solutions with two dark spots. Out of the four possible combinations, a good fit was only achieved when the two spots were located on the primary component⁴ The solutions with one dark spot on each component and two dark spots on the secondary yielded significantly poorer fits and were discarded. The configuration with two spots on the primary reproduces reasonably well the features observed in the light curves and results in root mean square residuals of 0.0087 mag and 0.0115 mag in R and I, respectively. Column 3 in Table 8 gives a summary of the light curve parameters resulting from this fit (spot scenario # 1). This solution, however, is unsatisfactory for a number of reasons: (i) the predicted luminosity ratios in each passband are significantly larger ($L_2/L_1 \approx 0.90 - 0.96$) than the values computed from the spectra of GU Boo (see §3.2 and Figure 3; $L_2/L_1 \approx 0.82 - 0.85$), (ii) the radius of the secondary (less massive) star is larger than the radius of the primary, which would be inconsistent with GU Boo being a main sequence system (see §5.2), and (iii) given the similarity in mass of the two components, it is difficult to explain how one star could be heavily spotted while the other one completely immaculate.

⁴The primary has been defined as the star eclipsed at orbital phase $\phi = 0.0$ in the light curves.

We tried some alternative scenarios to find a more physically realistic solution. Adding more dark spots did not improve the quality of the fits. We then considered a configuration with two spots but one of them being brighter than the surrounding photosphere (i.e. temperature factor greater than 1.0). After several tests we arrived at a configuration that yielded a fit of very similar quality to the two dark spot scenario described above. The root mean square residuals in this case are respectively 0.0086 mag in R and 0.0118 mag in I. The resulting orbital solution parameters are listed in column 4 of Table 8 (spot scenario # 2). This second fit is much more satisfactory because: (i) the luminosity ratios in the two passbands are in good agreement with the independent values found from the spectroscopic analysis, (ii) the radii of the stars are very similar and compatible with the expected ratio from a main sequence evolutionary stage, and (iii) the model predicts surface inhomogeneities (spots) in both stars. The resulting light curve fit is shown in Figure 4. A graphical representation of this spot configuration is shown in Figure 5. The photometric effects of the spots on the light curves are illustrated in Figure 6.

Being more physically valid, the only feature of this solution that needs further explanation is whether the presence of bright spots on the photosphere is realistic. This is not the first time that bright spots (plages) are suggested in low-mass binaries. Studies of YY Gem by Torres & Ribas (2002), Butler & Doyle (1996), and Kron (1952) mention possible *bright regions* to explain features observed in the light curves of that binary. Another case is that of the contact binary YY Eri (Maceroni et al. 1994). Moreover, a low-mass binary currently being analyzed by us (RXJ 0239.1-1028) shows indications of bright areas on the surface of the stars as well. We would like to mention, however, that bright spots on stellar surfaces can have an alternative explanation when only photometric data are being modeled. A light curve fitting program like WD2003 has a very simple spot model (circular, homogeneous spots) that is only able to measure the contrast between different areas on the surface of the star. The model of a star with a bright region at a certain location is equivalent to a model of the star with a dark area, of proportional temperature factor, covering the complementary surface. Thus, our scenario can be equivalently interpreted as a more or less uniform distribution of dark spots covering most of the stellar surface except for a spot-free area. This spot-free area can be modeled as a “bright spot” while, in reality, it represents the true photosphere. Fortunately, all this has no effect on the physical stellar properties but is just a reflex of the inherent indeterminacy of the spot models. It is only with future Doppler tomography studies of these binaries that the open question about the presence of bright surface homogeneities can be more conclusively addressed. In the meantime, we have decided to adopt this second scenario with a bright spot because it yields physically realistic parameters.

Note also that our model calls for the presence of large spots covering a significant

fraction of the stellar surfaces. The presence of such large spots is not a surprising result, given the high level of activity characteristic of low-mass stars. But a more realistic picture would be that of smaller groups of spots with larger temperature contrast distributed over the same surface area of the star covered by the single spot in the model (this has sometimes been referred to as a “starpatch”; see discussion in Toner & Gray 1988). In average, those groups of smaller spots would produce the same modulation in brightness as a single large spot with less contrast in temperature. The only difference is that an inhomogeneous distribution of small spot groups will cause rapid fluctuations in brightness as the spotted star undergoes eclipse and parts of the stellar surface with and without spots are gradually occulted. This kind of fluctuations is probably what we observe as larger residuals to the fits around the eclipses in Figure 4. Future very accurate photometry (for example from upcoming space missions) will improve the current coarse spot modeling by permitting detailed eclipse tomography.

Finally, there is a detail in Table 8 that deserves further discussion, which is the calculation of the stellar temperatures. The temperatures used by WD2003 correspond to the defined stellar (immaculate) photosphere. In cases where the spot areal coverage is small, this is a good representation of the overall effective temperature (i.e., related to the bolometric luminosity). However, in our case, spots cover a significant fraction of the stellar surfaces and thus the working temperatures in WD2003 deviate significantly from the stellar effective temperatures. We have therefore devised a procedure to calculate the effective temperature of a star with a large, either dark or bright, spot from its immaculate photospheric temperature. It is easy to demonstrate that the surface covered by a spot that subtends an angle of $2\theta_{\text{sp}}$ on a sphere of radius R is:

$$S_{\text{sp}} = 2\pi R^2(1 - \cos \theta_{\text{sp}}) \quad (2)$$

Then, the effective temperature (T_{eff}) is calculated from the photospheric temperature (T_{ph}) and the spot temperature (T_{sp}) using the areal coverage as the weighing factor:

$$T_{\text{eff}}^4 = \frac{S_{\text{sp}}T_{\text{sp}}^4 + S_{\text{ph}}T_{\text{ph}}^4}{S_{\text{tot}}} \quad (3)$$

This can be parameterized as a function of κ , which is the temperature factor ($T_{\text{sp}} = \kappa T_{\text{ph}}$), to obtain:

$$T_{\text{eff}} = \left(1 - \frac{(1 - \kappa^4)}{2}(1 - \cos \theta_{\text{sp}}) \right)^{1/4} T_{\text{ph}} \quad (4)$$

Using this expression we have corrected the working photosphere temperatures from WD2003 (in Table 8) to compute the effective temperatures for the components. To arrive at the final values 9 we adjusted the individual temperatures to yield the mean system temperature computed in §2.

5. The GU Boo System

5.1. Absolute Parameters of the Components

We used the parameters of the photometric and spectroscopic orbital solutions derived in the previous two sections to compute its absolute dimensions and physical parameters. The results are summarized in Table 9. The two stars in GU Boo are very similar, as their mass and radius ratios indicate. The ratio of the masses is $M_2/M_1 = 0.9832 \pm 0.0069$, while the ratio of the radii is $R_2/R_1 = 0.99 \pm 0.04$. The shape of the stars is practically spherical, with their radii being only $\simeq 3\%$ larger at the equator than at the poles (see values of the fractional radii in Table 8). This small elongation is caused by a combination of tidal interaction between the stars and rotational flattening effects.

The radius of each star is consistent with GU Boo being a main sequence system (see §5.2), and the larger error bars in R_2/R_1 result from the complications that the effects of spots introduce in the modeling of the light curves. Upcoming JHK photometry of GU Boo will give a second independent estimation of the radii of the stars by providing light curves GU Boo under a different spot configuration and at near-infrared wavelengths, where the effect of spots diminished with respect to the visible.

We derived the values of the projected rotational velocities of the stars from the orbital period of the binary (assuming synchronous rotation), and the radii of the stars in Table 9. The resulting projected rotational velocity of the primary, $v_{\text{sync}_1} \sin i = 64.4 \pm 1.6 \text{ km s}^{-1}$, agrees with the value estimated using TODCOR. In the case of the secondary, the resulting velocity $v_{\text{sync}_2} \sin i = 64.1 \pm 2.1 \text{ km s}^{-1}$ is 10% larger than the value of the best estimation from TODCOR. However, this discrepancy is consistent with the uncertainties in the radii that result from the fits to the light curves. We recomputed the radial velocities in TODCOR replacing the secondary template by a new template broadened by 64 km s^{-1} to find a variation of only 0.33% in the cross-correlation coefficient and no appreciable differences in the parameters of the binary derived from either radial velocity curve.

The relative difference in temperature of the two stars ($T_{\text{eff}_2}/T_{\text{eff}_1} = 0.972$) is consistent with the differences between their masses and between their radii. However, a more accurate determination of the mean absolute temperature of GU Boo is still necessary. The value adopted for the temperature of the primary in this work, $T_{\text{eff}_1} = 3920 \text{ K}$, is a preliminary estimation based on the average of the temperatures computed in §2. Note that the potentially large uncertainty in the effective temperature of the binary has no impact on the accuracy of the determined absolute dimensions. For example, the radii of the stars, which are obtained from the light curve modeling, suffer inappreciable changes when T_{eff} values $\pm 300 \text{ K}$ (2σ) about the mean are adopted.

The luminosity and absolute bolometric magnitudes M_{bol} of the stars in Table 9 were computed from their effective temperatures and their radii. We applied bolometric corrections BC_V to the M_{bol} of each star to derive their absolute visual magnitudes M_V . Those bolometric corrections were computed using the models in Table 2. The values obtained for each star are respectively, $BC_{V_1} = -1.14 \pm 0.08$ mag and $BC_{V_2} = -1.29 \pm 0.08$ mag. Finally, we have estimated a distance of $d \simeq 140 \pm 8$ pc for GU Boo from the distance modulus equation, using the joint absolute magnitude of the system $M_V = 7.98$ mag and assuming $m_V = m_{rotse} = 13.7$ mag.

5.2. Age and Space Velocities

An estimate of the age of GU Boo is an important parameter for a critical evaluation of stellar models. Such age estimation, however, is far from straightforward for low-mass stars because of their characteristic long evolution timescale. It is only during the pre-main sequence stage, which lasts for a few 10^8 yr (Chabrier & Baraffe 1995; Palla & Stahler 1999), that the properties of an M-type star suffer appreciable changes. Once on the main sequence, a stars with the masses of GU Boo will evolve at a very slow pace for tens of Gyr. Therefore, in our case, the key task is to find out whether the components of GU Boo could be in the pre-main sequence stage or if they have already arrived on the main sequence.

GU Boo appears to be an isolated system, not associated to any known cluster, stellar association, or star formation region. Therefore, a kinematic age estimate is the only possibility to evaluate whether the binary belongs in a young or old population. The relevant quantities for this study are the three components of the space velocity (U, V, W) ⁵. The heliocentric space velocity components of GU Boo were computed from its position, radial velocity ($\gamma = -24.57 \pm 0.36$ km s⁻¹; see Table 3), distance ($d = 140 \pm 8$ pc) and proper motions. The latter were retrieved from the USNO-B1.0 catalog (Monet et al. 2003): $\mu_\alpha = 26 \pm 4$ mas yr⁻¹; $\mu_\delta = -28 \pm 1$ mas yr⁻¹. The resulting space velocity components are: $U = 14.3 \pm 1.8$ km s⁻¹; $V = -12.6 \pm 1.5$ km s⁻¹; $W = -28.1 \pm 1.3$ km s⁻¹, which correspond to a total space velocity of $S = 34.0 \pm 2.7$ km s⁻¹.

We can infer from those space velocities whether GU Boo is a young population system (age < 300 Myr), which would imply a pre-main sequence stage, or if it has, on the contrary, parameters characteristic of an older population. There are a number of indications that favor the latter case and thus suggest that GU Boo has reached the main sequence: 1) The

⁵According to our convention, positive values of U , V , and W indicate velocities towards the galactic center, galactic rotation and North galactic pole, respectively.

location of the star on the UV plane does not fall within the area (although it lies not far from it) defined by Eggen (1984, 1987) as corresponding to the young disk population, nor in the area covered by young population tracers (Skuljan et al. 1999); 2) The space velocities do not match those of any known moving group (Montes et al. 2001); 3) The modulus value of the W velocity component (perpendicular to the Galactic plane) is significantly larger than expected for a young star ($W \approx -7 \pm 10 \text{ km s}^{-1}$; e.g. Mihalas & Binney 1981; Nordström et al. 2004), suggesting that GU Boo has been subject to “disk heating” processes, which operate over timescales longer than the galactic rotation period (200–250 Myr). There is always the possibility, however, of GU Boo being a young runaway object that has been ejected at relatively high velocity from its birthplace. In this case, its velocity would not correspond with its kinematic age. We cannot exclude this scenario with the current data but there is neither any indication favoring it. From the available evidence, we suggest that GU Boo is not a very young object and may possibly have an age of several gigayears. In addition, we do not expect the metal abundance of GU Boo to differ very significantly from the solar one, since the space motions are compatible with a disc population.

5.3. Stellar Activity Indicators

We provide here a comparison between some stellar activity indicators in GU Boo, and the same activity indication parameters observed in YY Gem and CU Cnc. In particular we focus on the $H\alpha$ and X-ray emission observed in the three objects. In the spectra of GU Boo collected to derive the radial velocity curves we observed clear evidences of strong emission in $H\alpha$. The observed emission features were double-peaked, and reached a maximum value of the continuum corrected equivalent widths of $\simeq 1.7 \pm 0.1 \text{ \AA}$ at orbital phase $\phi \simeq 0.01$ (around primary eclipse). There was no apparent correlation between the phase of the maximum $H\alpha$ emission in the spectra and the phase of the spots in the light curves, although the reason for this is that each dataset was collected in a different epoch. The observed levels of $H\alpha$ emission in GU Boo are lower than the emission levels in YY Gem ($\simeq 2 \text{ \AA}$) and CU Cnc (3.85 \AA and 4.05 \AA) reported by Young et al. (1989) and Ribas (2003), respectively.

GU Boo also appears in the ROSAT All-Sky Bright Source Catalog (Voges et al. 1999), as X-ray source 1RXS J152155.7+335625. Using the calibration equation by Schmitt et al. (1995) we have estimated an X-ray luminosity of $\log L_X \text{ (ergs s}^{-1}\text{)} = 29.3 \pm 0.2$ for GU Boo, which is very similar to the X-ray luminosity of YY Gem, $\log L_X \text{ (ergs s}^{-1}\text{)} = 29.27 \pm 0.02$, computed using the same calibration equation and the parameters of this binary from ROSAT. This result indicates that the levels of X-ray activity for both systems are very similar. Furthermore, the fact that the estimated X-ray luminosity of GU Boo agrees

with that of YY Gem indicates consistency with the distance of 140 ± 8 pc derived above.

6. Comparison with Models

We compare in this section the masses and radii of the components of GU Boo to the predictions by the models of Pietrinferni et al. (2004), Yi et al. (2001), Girardi et al. (2000), Baraffe et al. (1998), D’Antona & Mazzitelli (1997), and Siess et al. (1997). This list of models, although not complete, provides a representative sample of the predictions by all current models. The models by Baraffe et al. (1998) and Siess et al. (1997) are in fact the only ones that explicitly attempt to reproduce the properties of main sequence low-mass stars. The models by D’Antona & Mazzitelli (1997) focus on the pre-main sequence stage, and only include isochrones up to 0.5 Gyr. The rest of the models, designed for more massive stars, are not expected to reproduce the observations very well, but we include them here to illustrate their behavior versus the observations. For completeness, we also compare the observed mass- $\log T_{\text{eff}}$, mass- M_V , and $\log T_{\text{eff}}-M_V$ relations of GU Boo to the predictions by the models. We also include in these comparisons the other known low-mass binaries, whose parameters are listed in Table 10.

Given that the metal abundance of GU Boo is currently undetermined, we considered models for two different metallicities, $Z= 0.01$ and $Z= 0.02$ (we expect the metallicity of GU Boo to be close to solar, as explained in §5.2). We also considered two main-sequence isochrone ages in the mass-radius relation (Figure 7), after concluding from the space velocities computed in §5.2 that the system has most likely already reached the main sequence stage. The age of the isochrones are 0.35 and 3.0 Gyr, respectively⁶. In the figures representing the mass- $\log T_{\text{eff}}$, mass- M_V , and $\log T_{\text{eff}}-M_V$ relations (Figures 8, 9, and 10) we opted for showing only the 0.35 Gyr isochrones, after verifying that both the 0.35 and 3.0 Gyr isochrones produce, as expected, practically identical results. Using the 0.35 Gyr isochrones allows us to directly compare the parameters of GU Boo to those of YY Gem and CU Cnc, whose ages have been estimated to be of the order of 320–370 Myr (Torres & Ribas 2002; Ribas 2003).

Figure 7 shows the comparison of the masses and radii of GU Boo to the different mass-radius relations predicted by the six models considered in this analysis. Each column in the figure represents a different age (0.35 Gyr on the left, and 3.0 Gyr on the right), and each row

⁶Chabrier & Baraffe (1995) have estimated a time of arrival to the ZAMS of about 0.3 Gyr for stars of $\sim 0.6 M_{\odot}$. Therefore both the 0.35 and 3.0 Gyr isochrones represent stars that have already reached the main sequence stage.

represents a different metallicity (0.01 at the top, and 0.02 at the bottom). Details about the parameters of each model are listed in Table 11. The open circles in each plot show the location of the two components of GU Boo. In diagram c) we also include the location of the components of YY Gem (filled circle coincident with the less massive component of GU Boo), CU Cnc (open triangles), and BW3 V38 (crosses). The age and metallicity in that diagram (Age=0.35 Gyr; Z=0.02) resemble the age and metallicity of YY Gem and CU Cnc estimated by Torres & Ribas (2002) and Ribas (2003), respectively. The stars in BW3 V38 are included only for completeness, since the current uncertainties of the parameters of this system are too large to place any strong constraint in the models. Finally, we have not included CM Dra in that diagram since that binary is believed to be an older Population II system.

We find that all the models consistently predict smaller radii than the ones observed, independently of age and metallicity. The discrepancies between the models and the observations are of the order of 10–15%. This result fully agrees with the trend observed in the components of YY Gem and CU Cnc by Torres & Ribas (2002) and Ribas (2003).

In Figures 8, 9, and 10 we compare, respectively, the mass- $\log T_{\text{eff}}$, mass- M_V , and $\log T_{\text{eff}}-M_V$ relations of GU Boo again to the predictions by the models. The isochrones in this case are for a single age of 0.35 Gyr (the 3.0 Gyr isochrones give practically identical results). We consider again the two values of the metallicity Z= 0.01 and Z= 0.02. The bottom diagrams in each figure (age= 0.35 Gyr, Z= 0.02) include YY Gem and CU Cnc for comparison

The error bars of the absolute magnitudes and effective temperatures in these plots are relatively larger than the errors in the masses and radii in Figure 7. This is a consequence of the need to use external calibrations to compute T_{eff} and M_V , whereas M and R are measured directly from the light and radial velocity curves. Because of the larger errors, the data in the mass- $\log T_{\text{eff}}$, mass- M_V , and $\log T_{\text{eff}}-M_V$ relations do not provide as strong constraints on the models as the mass-radius relation in Figure 7. However, we can still study whether significant discrepancies between models and observations exist.

The mass- $\log T_{\text{eff}}$ relations in Figure 8 show that such discrepancies indeed exist between the effective temperatures of GU Boo and the temperatures predicted by the models, especially in the case of Z = 0.01. In the case of Z = 0.02, there is better agreement between models and observations, although the majority of the models still overestimate the stellar temperatures by several hundred degrees. Only the models by Baraffe et al. (1998) give rather close values to the effective temperatures of GU Boo. Although this latter model does not reproduce the temperatures of the individual stars, it does predict a value of $T_{\text{eff}} = 3890$ K for an intermediate mass of $0.6 M_{\odot}$, which agrees with the mean effective temperature of GU Boo derived in §2 ($T_{\text{eff}} = 3870 \pm 130$ K). The figure also shows that the effective

temperatures of GU Boo are very similar to the values derived for YY Gem by Torres & Ribas (2002).

In the case of the mass- M_V relations (Figure 9), the $Z = 0.02$ models are again the ones reproducing more closely the observations, although none of them provides an exact match to the estimated absolute magnitudes of GU Boo. There is only a slight difference between the absolute magnitude of YY Gem ($M_V = 8.95 \pm 0.03$; Torres & Ribas 2002) and the absolute magnitude of the almost identical secondary in GU Boo. Such slight difference indicates no large systematic errors between the two methods used to compute the magnitudes of each binary. The absolute magnitudes of YY Gem were computed by Torres & Ribas (2002) using the Hipparcos parallax of stars in the Castor group (YY Gem is thought to be part of it), while the absolute magnitudes of GU Boo were derived using bolometric corrections from models (see §5.1). The Baraffe et al. (1998) models reproduce well the absolute magnitude of YY Gem, but slightly underestimate the magnitudes of GU Boo.

Finally, the comparison in Figure 10 of the $\log T_{\text{eff}}-M_V$ diagram of GU Boo with the models leads to the same conclusions as Figures 8 and 9. This is because the $\log T_{\text{eff}}-M_V$ relation is just a combination of the relations in those two figures. For a given temperature all the $Z = 0.02$ models (which produce the best agreement) overestimate the effective temperature of the stars, with Baraffe et al. (1998) being the models that yield the closest match to the observations.

7. Summary and Conclusions

We report in this paper the finding of GU Boo, a new double-lined, detached eclipsing binary composed of two M-type stars. We have performed a detailed analysis of complete R- and I-band light curves and radial velocity curves of the system to derive its absolute physical stellar parameters, such as the masses $M_1 = 0.610 \pm 0.007 M_\odot$, $M_2 = 0.599 \pm 0.006 M_\odot$, and radii $R_1 = 0.623 \pm 0.016 R_\odot$, $R_2 = 0.620 \pm 0.020 R_\odot$. The uncertainties of the derived radii of the GU Boo components ($\sim 3\%$) are somewhat larger than expected from the quality of the light curves. This is because of the complications in the modeling caused by presence of large *spots* on the surface of the stars. We are in the process of collecting new light curves at near-infrared wavelengths, which are much less affected by spots, which will allow us to refine the current radius measurements. The effective temperatures of the components have been estimated to be $T_{\text{eff}1} = 3920 \pm 130$ K and $T_{\text{eff}2} = 3810 \pm 130$ K from the observed photometry and by means of both empirical and model-dependent calibrations. In addition, we have used the space velocities of the binary to conclude that GU Boo is most likely in its main sequence evolutionary phase, with an estimated age of several gigayears.

Therefore, the parameters of the stars in GU Boo should be suitable to test stellar structure models.

The stars in GU Boo are very similar to the components of YY Gem. This eclipsing binary, together with CU Cnc and CM Dra, were to date the only simultaneous measurements of stellar masses and radii of M-type main sequence stars, with uncertainties of less than 3%. The measurements from those three binaries were until now the only available data points to provide critical constraints to low-mass stellar models. The addition of the two masses and radii from the stars in GU Boo therefore increases by 40% the number of accurate measurements in that mass regime.

The comparison of the masses and radii of GU Boo with several current low-mass models of stellar structure corroborates the results of similar studies of YY Gem and CU Cnc by Torres & Ribas (2002) and Ribas (2003). That is, the radii of the stars in this mass domain are at least 10–15% larger than the predictions by any of the models. We arrived to the same result independently of the adopted metallicity of the system. The models that provide a better fit to the observations are those of Baraffe et al. (1998), for a metallicity of $Z = 0.02$, although a noticeable underestimation of the observed radii is still present. Note that the metallicity of GU Boo is presently undetermined. This, however, does not alter our conclusions about the radius discrepancy because of the relative insensitivity of this parameter to the metallicity. The radii of the stars are mainly determined by the interior equation of state and depend only weakly on the atmospheric properties, where the metallicity plays the most important role. The mass-radius relation is therefore providing us with direct information about the interior conditions of low-mass stars.

Following this reasoning, the radius discrepancies between the predictions of the models and the observations might be, in principle, attributable to inaccuracies in the equation of state. However, the models successfully describe the masses and luminosities of the eclipsing binary components and also of stars in non-eclipsing spectroscopic binaries (e.g., Delfosse et al. 2000). This apparent paradox can be explained if the stars have larger radius and cooler temperature than predicted by models but just in the right proportions. That is, the 10–15% radius underestimation compensated by a 5–7% temperature overestimation to yield identical luminosities.

In all the comparisons with models we assume that the eclipsing binary sample available thus far is representative of the overall M star population. Because of the presence of discrepancies between models and theory it is worth reviewing this assumption. The three eclipsing binaries used in the model comparison are well-detached systems with components that have not suffered major interactions through mass exchange. There is, however, one difference with respect to field stars and stars in wide binaries, which is the relative fast

rotation rate caused by orbital synchronization (periods of 0.5–2.8 days). This high rotational velocity gives rise to enhanced magnetic activity and thus to the appearance of surface inhomogeneities, emission lines and X-ray fluxes. All these phenomena are observed at their peak (saturated activity; Vilhu & Walter 1987; Stauffer et al. 1994) in YY Gem, CU Cnc and GU Boo. It might be speculated that the larger radii and lower temperatures could be a reflex of such enhanced activity. Perhaps the significant spot areal coverage observed in the three eclipsing systems has the effect of lowering the overall photospheric temperature, which the star compensates by increasing its radius to conserve the total radiative flux.

If this scenario turns out to be correct, and there is a correlation between the radius and the activity level of an M-type star, the consequences are far reaching. Young low-mass stars are known to be very active because they are generally fast rotators (e.g., Pizzolato et al. 2003). Then, they lose angular momentum via magnetic braking and spin down with age. Thus, the radius discrepancy would not only affect the components of close binaries but any active field M-type star, including those in young clusters. Only old, inactive M stars (e.g., in the halo) might have observed and predicted radii in agreement, but no observations are available for a check.

Clearly, more observational data (in the form of a large sample of eclipsing binaries with different rotational velocities) and careful modeling are needed to validate this scenario. This paper summarizes the first results of an ongoing effort to provide a well-sampled empirical mass-radius relation of stars below $1 M_{\odot}$ using detached eclipsing binaries. Our current sample consists of over a dozen new binaries with components between ~ 0.35 – $1.0 M_{\odot}$, and orbital periods of less than 2.5 days. The resulting ensemble of stars will provide valuable tests to low-mass stellar models that should help to resolve the current lingering discrepancies between observations and theory.

8. Acknowledgments

We would like to thank Dr. Scott Shaw from the University of Georgia in Athens, and the Southeastern Association for Research in Astronomy (SARA) Observatory for making their allocated telescope time and their facilities available to us. We give special thanks to Dr. Chris Clemens from the University of North Carolina at Chapel Hill for his useful advise in the initial parts of this work. We are also grateful to Drs. Latham and Torres from CfA-Harvard for their hospitality and for allowing us to used their implementation of TODCOR. We thank Dr. David Fernández for his comments and help on performing the kinematic analysis of GU Boo. M. L-M. acknowledges research and travel support from the Carnegie Institution of Washington through a Carnegie Fellowship. I. R. acknowledges

support from the Spanish Ministerio de Ciencia y Tecnología through a Ramón y Cajal Fellowship. An anonymous referee is thanked for a number of useful comments and suggestions. This publication makes use of data products from the Two Micron All Sky Survey, which is a joint project of the University of Massachusetts and the Infrared Processing and Analysis Center/California Institute of Technology, funded by the National Aeronautics and Space Administration and the National Science Foundation. This project has been partially supported by the National Science Foundation through grant AST 00-94289.

REFERENCES

- Akerlof, C., Amrose, S., Balsano, R., Bloch, J., Casperson, D., Fletcher, S., Gisler, G., Hills, J., Kehoe, R., Lee, B., Marshall, S., McKay, T., Pawl, A., Schaefer, J., Szymanski, J. & Wren, J. 2000, *AJ*, 119, 1901
- Allard, F. & Hauschildt, P. H. 1995, *ApJ*, 445, 433
- Allard, F., Hauschildt, P. H., Alexander, D. R., & Starrfield, S. 1997, *ARA&A*, 35, 137
- Arribas, S. & Martínez Roger, C. 1989, *A&A*, 215, 305
- Baraffe, I., Chabrier, G., Allard, F., & Hauschildt, P.H. 1998, *A&A*, 337, 403
- Bell, S. A., Rainger, P. P. & Hilditch, R. W. 1990, *MNRAS*, 247, 632
- Bessel, M. S. 1979, *PASP*, 91, 589
- Bessell, M. S., Castelli, F., & Plez, B. 1998, *A&A*, 333, 231
- Butler, C. J. & Doyle, J. G. 1996, in *ASP Conf. Ser. 109, Cool Stars, Stellar Systems, and the Sun, 9th Cambridge Workshop*, ed. R. Pallavicini & A. K. Dupree (San Francisco: ASP), 589
- Chabrier, G. & Baraffe, I. 1995, *ApJ*, 451, L29
- Chabrier, G. & Baraffe, I. 2000, *ARA&A*, 38, 337
- Claret, A. 2000, *A&A*, 363, 1081
- Creevey, O. L., Benedict, G. F, Brown, T. R., et al. 2005, *ApJL*, in press
- Cutri, R. M. et al. 2003, *The 2MASS All-Sky Catalog of Point Sources*, University of Massachusetts and Infrared Processing and Analysis Center, IPAC/California Institute of Technology.

- D'Antona, F. & Mazzitelli, I. 1997, *Mem. Soc. Astron. Italiana*, 68, 807
- Delfosse, X., Forveille, T., Mayor, M., Burnet, M., & Perrier, C. 1999, *A&A* 341, L63
- Delfosse, X., Forveille, T., Ségransan, D., Beuzit, J.-L., Udry, S., Perrier, C., Mayor, M. 2000, *A&A*, 364, 217
- Diaz-Cordovés, J. & Giménez, A. 1992, *A&A*, 259, 227
- Diethelm, R. 2001, *Information Bulletin on Variable Stars*, 5060, 1
- Eggen, O. 1984, *ApJS*, 55, 597
- Eggen, O. 1987, *PASP*, 101, 366
- Girardi, L., Bressan, A., Bertelli, G., & Chiosi, C. 2000, *A&AS*, 141, 371
- Gliese, W. & Jahreiss, H. 1991, *Preliminary Version of the Third Catalogue of Nearby Stars*, Astron. Rechen-Institut (Heidelberg: Germany)
- Granzer, T., Schüssler, M., Caligari, P., & Strassmeier, K. G. 2000, *A&A*, 355, 1087
- Hatzes, A. P. 1995, in *IAU Symp. 176, Stellar Surface Structure*, ed. K. G. Strassmeier (Vienna: Institut für Astronomie), 90
- Hauschildt, P. H., Allard F., & Baron, E. 1999, *ApJ*, 512, 377
- Henry, T. J. & McCarthy, D. W. Jr. 1993, *AJ*, 106, 773
- Kallrath, J. & Milone, E. F. 1999, *Eclipsing Binary Stars: Modeling and Analysis*, Springer-Verlag New York Inc., New York
- Kazarovets et al. 2003, *Information Bulletin on Variable Stars*, 5422, 1
- Kron, G. E. 1952, *ApJ*, 115, 301
- Lacy, C. H. 1977, *ApJ*, 218, 444
- Lasker et al. 1996, *Guide Star Photometric Catalog*
- Lejeune, T., Cuisinier, F., & Buser, R. 1998, *A&AS*, 130, 65
- Leung K.C. & Schneider, D.P. 1978, *AJ*, 83, 618
- López-Morales, M. & Clemens, J. C. 2004, *PASP*, 116, 22

- Maceroni, C. & Montalbán, J. 2004, *A&A*, 426, 577
- Maceroni, C., Vilhu, O., van't Veer, F. & van Hamme, W. 1994, *A&A*, 288, 529
- Maceroni, C. & van't Veer, F. 1993, *A&A*, 277, 515
- Metcalfe, T. S., Mathieu, R. D., Latham, D. W., & Torres, G. 1996, *ApJ*, 456, 356
- Mihalas, D., & Binney, J. 1981, "Galactic Astronomy" (W. H. Freeman and Co.: New York)
- Monet, D. G., Harris, H., Reid, N., Rhodes, A. & Sell, S. 1997, The USNO-A1.0 Catalog
- Monet, D. G. et al. 2003, *AJ*, 125, 984, The USNO-B1.0 Catalog
- Montes, D., López-Santiago, J., Gálvez, M. C., Fernández-Figueroa, M.J., De Castro, E., & Cornide, M. 2001, *MNRAS*, 328, 45
- Nordström, B., Mayor, M., Andersen, J., Holmberg, J., Pont, F., Jørgensen, B. R., Olsen, E. H., Udry, S., & Mowlavi, N. 2004, *A&A*, 418, 989
- Palla, F., & Stahler, S. W. 1999, *ApJ*, 525, 772
- Pietrinferni, A., Cassisi, S., Salaris, M., & Castelli, F. 2004, *ApJ*, 612, 168
- Pizzolato, N., Maggio, A., Micela, G., Sciortino, S., & Ventura, P. 2003, *A&A*, 397, 147
- Ribas, I. 2003, *A&A*, 398, 239
- Schmitt, J. H. M. N., Fleming, T. A., & Giampapa, M. S. 1995, *ApJ*, 450, 392
- Skuljan, J., Hearnshaw, J. B., & Cottrell, P. L. 1999, *MNRAS*, 308, 731
- Siess, L., Forestini, M., & Dougados, C. 1997, *A&A*, 324, 556
- Stauffer, J. R., Caillault, J.-P., Gagne, M., Prosser, C. F., & Hartmann, L. W. 1994, *ApJS*, 91, 625
- Toner, C. G., & Gray, D. F. 1988, *ApJ*, 334, 1008
- Torres, G. & Ribas, I. 2002, *ApJ*, 567, 1140
- Van Hamme, W., Samec, R. G., Gothard, N. W., Wilson, R. E., Faulkner, D. R. & Branly, R. M. 2001, *AJ*, 122, 3436
- Vilhu, O., & Walter, F. M. 1987, *ApJ*, 321, 958

Voges, W., Aschenbach, B., Boller, T. et al. 1999, *A&A*, 349, 389

Wilson, R. E. & Devinney, E. J. 1971, *ApJ*, 166, 605

Yi, S., Demarque, P., Kim, Y. C., Lee, Y. W., Ree, C. H., Lejeune, T., & Barnes, S. 2001, *ApJS*, 136, 417

Young, A., Skumanich, A., Stauffer, J. R., Harlan, E., & Bopp, B. W. 1989, *ApJ*, 344, 427

Zucker, S. & Mazeh, T. 1994, *ApJ*, 420, 806

Table 1: Magnitudes of GU Boo collected from the literature

Bandpass	Magnitude	Source
V_{rotse}	13.7	Akerlof et al. (2000)
I	11.80 ± 0.05	This work ^a
b	15.0	USNO-A1.0 Catalog (Monet et al. 1997)
r	13.2	USNO-A1.0 Catalog (Monet et al. 1997)
B1	15.18	USNO-B1.0 Catalog (Monet et al. 2003)
R1	13.12	USNO-B1.0 Catalog (Monet et al. 2003)
$J_{2\text{MASS}}$	11.046 ± 0.024	2MASS All-Sky Catalog of Point Sources (Cutri et al. 2003)
$H_{2\text{MASS}}$	10.362 ± 0.030	2MASS All-Sky Catalog of Point Sources (Cutri et al. 2003)
$K_{2\text{MASS}}$	10.222 ± 0.021	2MASS All-Sky Catalog of Point Sources (Cutri et al. 2003)

^aUsing the 0.2-m Pisgah Survey robotic telescope (López-Morales & Clemens 2004) equipped with an I-band filter.

Table 2: Mean effective temperature estimations of GU Boo

Empirical calibrations	Color Indexes	T_{eff} (K)
Arribas & Martínez Roger (1989)	(V-K)	4040
Bessell (1979)	(V-I), (R-I), (B-V)	3760
Model-dependent calibrations	Color Indexes	T_{eff} (K)
Bessel et al. (1998)	(V-I), (V-K), (J-K)	3835
Lejeune et al. (1998)	(V-I), (V-K)	3760
Hauschildt et al. (1999)	(V-I), (V-K), (J-K)	3900

Table 3: Parameters of GU Boo derived from the orbital solution of the radial velocity curves

Element	Value
Adjusted quantities:	
P (days)*	0.4887280
γ (km s ⁻¹)	-24.57 ± 0.36
K_1 (km s ⁻¹)	142.65 ± 0.66
K_2 (km s ⁻¹)	145.08 ± 0.73
e*	0.0000
T_o (HJD)	2452723.9811
Derived quantities:	
$M_1 \sin^3 i$ (M_\odot)	0.6082 ± 0.0067
$M_2 \sin^3 i$ (M_\odot)	0.5980 ± 0.0063
$q \equiv M_2/M_1$	0.9832 ± 0.0069
$a_1 \sin i$ (10 ⁶ km)	0.9587 ± 0.0045
$a_2 \sin i$ (10 ⁶ km)	0.9750 ± 0.0049
Other quantities:	
N_{obs}	103
Time span (days)	9.30
N_{cycles}	19.0
σ_1 (km s ⁻¹)	4.77
σ_2 (km s ⁻¹)	5.24

*Parameter fixed beforehand

Table 4: Radial velocity measurements

HJD	Orbital phase	RV_1 kms ⁻¹	RV_2 km s ⁻¹	$(O - C)_1$ km s ⁻¹	$(O - C)_2$ km s ⁻¹
2452769.6797	0.505	-28.27	-26.97	-7.86	1.83
2452769.6841	0.514	-7.43	-36.39	4.92	0.60
2452769.6867	0.520	5.39	-39.76	13.00	2.05
2452769.6892	0.525	3.23	-49.02	6.30	-2.59
2452769.6918	0.530	14.17	-49.33	12.54	1.88
...

Table 5: Times of minima measured from the R- and I-band light curves

E	Min Type*	HJD	(O-C) (days)
0	p	2452723.98143	+0.00035
2	p	2452724.95853	-0.00001
18	p	2452732.77768	-0.00051
21	s	2452734.00061	+0.00060
53	p	2452749.88383	+0.00017
80	s	2452762.83524	+0.00028
86	s	2452765.76735	+0.00002

*p = primary; s = secondary.

Table 6: Date, phase coverage, and number of observations per phase interval of the light curve observations

Filter	HJD-2450000	Orbital phase	# of Obs.
R	2733.753–2734.029	0.996–0.559	107
R	2749.756–2750.007	0.685–0.253	163
R	2765.669–2765.811	0.301–0.901	95
I	2724.873–2725.029	0.825–0.145	190
I	2732.767–2733.029	0.977–0.514	178
I	2762.688–2762.952	0.201–0.741	254

Table 7: R-band light curve measurements

HJD	Orbital phase	Differential mag.
2452733.75358	0.996	0.222
2452733.75571	0.000	0.152
2452733.75903	0.007	0.206
2452733.76210	0.014	0.296
2452733.76833	0.026	0.498
2452733.77785	0.046	0.735
2452733.78065	0.051	0.783
2452733.78310	0.056	0.827
...

Table 8: Parameters of GU Boo for two spot scenarios

	Parameter	Spot Scenario # 1	Spot Scenario # 2	Fixing [†]
Geometric parameters:	P (days)*	0.4887280	0.4887280	[1]
	e*	0.0000	0.0000	[1]
	$\Delta\phi$	0.0012 \pm 0.0002	0.00007 \pm 0.00002	
	i (deg)	88.2 \pm 0.2	87.6 \pm 0.2	
	Ω_1	5.523 \pm 0.118	5.382 \pm 0.112	
	Ω_2	5.636 \pm 0.112	5.427 \pm 0.105	
	q = M_2/M_1 *	0.9832	0.9832	[1]
Fractional radii of primary	$r_{1\text{point}}$	0.2256 \pm 0.0016	0.2292 \pm 0.0016	
	$r_{1\text{pole}}$	0.2188 \pm 0.0014	0.2220 \pm 0.0018	
	$r_{1\text{side}}$	0.2211 \pm 0.0015	0.2244 \pm 0.0015	
	$r_{1\text{back}}$	0.2243 \pm 0.0016	0.2279 \pm 0.0016	
	$r_{1\text{**}}$	0.221 \pm 0.005	0.224 \pm 0.005	
Fractional radii of secondary	$r_{2\text{point}}$	0.2366 \pm 0.0014	0.2282 \pm 0.0021	
	$r_{2\text{pole}}$	0.2281 \pm 0.0012	0.2209 \pm 0.0018	
	$r_{2\text{side}}$	0.2309 \pm 0.0013	0.2234 \pm 0.0019	
	$r_{2\text{back}}$	0.2349 \pm 0.0014	0.2268 \pm 0.0020	
	$r_{2\text{**}}$	0.231 \pm 0.004	0.223 \pm 0.006	
Radiative parameters:	Gravity brightening*	0.2	0.2	[2]
	$T_{\text{ph}1}$ (K)*	4050	3940	[4]
	$T_{\text{ph}2}$ (K)	3820 \pm 10	3800 \pm 10	
	Albedo*	0.5	0.5	[2]
Light ratio (R-band)	L_2/L_1 ***	0.90 \pm 0.04	0.80 \pm 0.04	
Light ratio (I-band)	L_2/L_1 ***	0.96 \pm 0.03	0.85 \pm 0.03	
Limb darkening coefficients * : (square-root law):	$x_{\text{bol}1}, y_{\text{bol}1}$	0.207, 0.665	0.210, 0.662	[2]
	$x_{\text{bol}2}, y_{\text{bol}2}$	0.192, 0.719	0.201, 0.695	[2]
	($x_{\text{R}1}, y_{\text{R}1}$)	0.607, 0.212	0.617, 0.202	
	($x_{\text{R}2}, y_{\text{R}2}$)	0.463, 0.369	0.510, 0.316	
	($x_{\text{I}1}, y_{\text{I}1}$)	0.193, 0.618	0.201, 0.610	
	($x_{\text{I}2}, y_{\text{I}2}$)	0.059, 0.784	0.095, 0.736	
Spot 1 parameters:	Star Location ..	Primary	Primary	
	Latitude (deg)*	45	63	[2],[3]
	Longitude (deg)	349	349	
	Angular radius (deg)	89	33	
	$T_{\text{spot}}/T_{\text{surf}}$ *	0.95	0.94	[4]
Spot 2 parameters:	Star Location	Primary	Secondary	
	Latitude (deg)*	45	63	[2],[3]
	Longitude (deg)	153	22	
	Angular radius (deg)	43	23	
	$T_{\text{spot}}/T_{\text{surf}}$ *	0.94	1.06	[4]
rms residuals	R-band	0.0087	0.0086	
	I-band	0.0115	0.0118	

[†][1]: Parameter fixed by the orbital solution of the radial velocity curve; [2]: Parameter fixed from the literature; [3]: Parameter fixed from preliminary solutions of WD2003; [4]: Other sources (see text).

*Parameters fixed in the final computation of the orbital solution (see explanation in the text).

**Volume radius.

***Out-of-eclipse average (phase intervals: 0.075-0.427 & 0.574-0.927).

Table 9: Absolute dimensions and main physical parameters of the components of GU Boo

Parameter	Primary	Secondary
Mass (M_{\odot})	0.610 ± 0.007	0.599 ± 0.006
Radius (R_{\odot})	0.623 ± 0.016	0.620 ± 0.020
$\log g$ (cgs)	4.634 ± 0.023	4.630 ± 0.028
$v_{\text{sync}} \sin i$ (km s $^{-1}$)	64.43 ± 1.65	64.15 ± 2.07
T_{eff} (K)	3920 ± 130	3810 ± 130
L/L_{\odot}	0.082 ± 0.011	0.073 ± 0.013
M_{bol} (mag)	7.46 ± 0.15	7.60 ± 0.16
M_V (mag)	8.60 ± 0.17	8.89 ± 0.18

NOTES – The luminosities and bolometric magnitudes were computed from the radii and the effective temperatures, using $M_{\text{bol}}^{\odot} = 4.72$ and $T_{\text{eff}}^{\odot} = 5778$ K. The absolute magnitudes M_V were computed using bolometric corrections derived from the models in Table 11.

Table 10: Summary of the main physical parameters of the six M-type eclipsing binaries studied to date.

Binary	Parameter	Primary	Secondary	Reference
YY Gem	Mass (M_{\odot})	0.5992 ± 0.0047	0.5992 ± 0.0047	[a]
	Radius (R_{\odot})	0.6191 ± 0.0057	0.6191 ± 0.0057	[a]
	T_{eff} (K)	3820 ± 100	3820 ± 100	[a]
	M_V	8.950 ± 0.029	8.950 ± 0.029	[a]
BW3 V38	Mass (M_{\odot})	0.44 ± 0.07	0.41 ± 0.09	[b]
	Radius (R_{\odot})	0.51 ± 0.04	0.44 ± 0.06	[b]
	T_{eff} (K)	3500*	3448 ± 11	[b]
TrES-Her0 ...	Mass (M_{\odot})	0.493 ± 0.003	0.489 ± 0.003	[c]
	Radius (R_{\odot})	0.453 ± 0.060	0.452 ± 0.050	[c]
CU Cnc	Mass (M_{\odot})	0.4333 ± 0.0017	0.3890 ± 0.0014	[d]
	Radius (R_{\odot})	0.4317 ± 0.0052	0.3908 ± 0.0094	[d]
	T_{eff} (K)	3160 ± 150	3125 ± 150	[d]
	M_V	11.95 ± 0.16	12.31 ± 0.16	[d]
CM Dra	Mass (M_{\odot})	0.2307 ± 0.0010	0.2136 ± 0.0010	[e]
	Radius (R_{\odot})	0.2516 ± 0.0020	0.2347 ± 0.0019	[e]
GU Boo	Mass (M_{\odot})	0.610 ± 0.007	0.599 ± 0.006	[f]
	Radius (R_{\odot})	0.623 ± 0.016	0.620 ± 0.020	[f]
	T_{eff} (K)	3920 ± 130	3810 ± 130	[f]
	M_V	8.60 ± 0.17	8.89 ± 0.18	[f]

NOTES – [a] Torres & Ribas (2002), [b] Maceroni & Montalbán (2004), [c] Creevey et al. (2005), [d] Ribas (2003), and [e] Metcalfe et al. (1996). The last entries correspond to parameters of the newest binary, GU Boo, analyzed in this work (reference [f]).

Table 11: Summary of the parameters of the models used in the M–R, M– $\log T_{eff}$, M– M_V , and $\log T_{eff}$ – M_V relations

Model ID	Reference	M_{\min} [M_{\odot}]	M_{\max} [M_{\odot}]	Y	Age [Gyr]	Z_1 (=0.01)	Z_2 (=0.02)	Notes (*)
[1]	Yi et al. (2001)	0.4	1.0	*	0.35	✓	✓	$Y_{Z_2}=0.250$
				*	3.00	✓	✓	$Y_{Z_3}=0.270$
[2]	Baraffe et al. (1998)	0.075	1.0	0.275	0.35	—	✓	...
				0.275	3.00	—	✓	...
[3]	Siess et al (1997)	0.1	1.0	*	0.35	✓	✓	$Y_{Z_2}=0.256$
				*	3.00	✓	✓	$Y_{Z_3}=0.277$
[4]	D’Antona et al. (1997)	0.02	1.0	*	0.35	✓	✓	$Y_{Z_2}=0.260$
				*	3.00	—	—	$Y_{Z_3}=0.280$
[5]	Girardi et al. (2000)	0.15	1.0	*	0.35	✓	✓	$Z_2=0.008; Y_{Z_2}=0.250$
				*	3.00	✓	✓	$Z_3=0.019; Y_{Z_3}=0.273$
[6]	Pietrinferni et. al (2004)	0.5	1.0	*	0.35	✓	✓	$Y_{Z_2}=0.259$
				*	3.00	✓	✓	$Z_3=0.0198; Y_{Z_3}=0.273$

NOTE – M_{\min} and M_{\max} correspond to the minimum and maximum stellar mass simulated by the models in the figure, Y is the He abundance, and the check marks (or crossed lines) under the values of the metallicities Z_1 and Z_2 indicate whether or not isochrones for that particular metallicity are available.

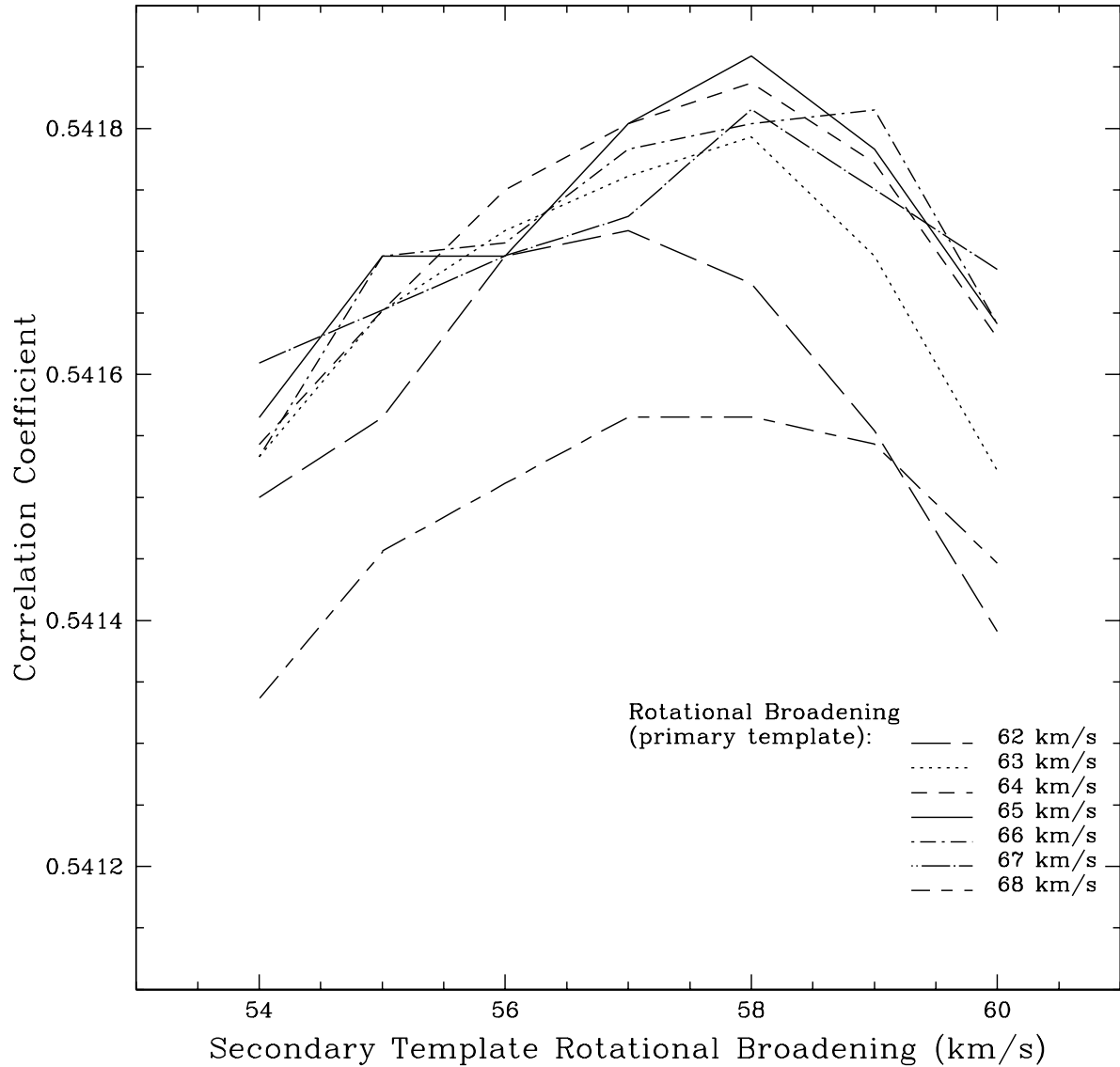


Fig. 1.— Variation of the correlation coefficient in TODCOR as a function of the rotational broadening of the template of the secondary. We use the spectra of GJ 410 as template for both the primary and the secondary. Each curve in the figure corresponds to a fixed value of the rotational broadening of the primary template (see values in the lower-right corner). The values of the broadening of the secondary are represented in the horizontal axis. The highest value of the correlation coefficient in TODCOR corresponds to rotational broadenings of 65 km s^{-1} for the primary, and 58 km s^{-1} for the secondary.

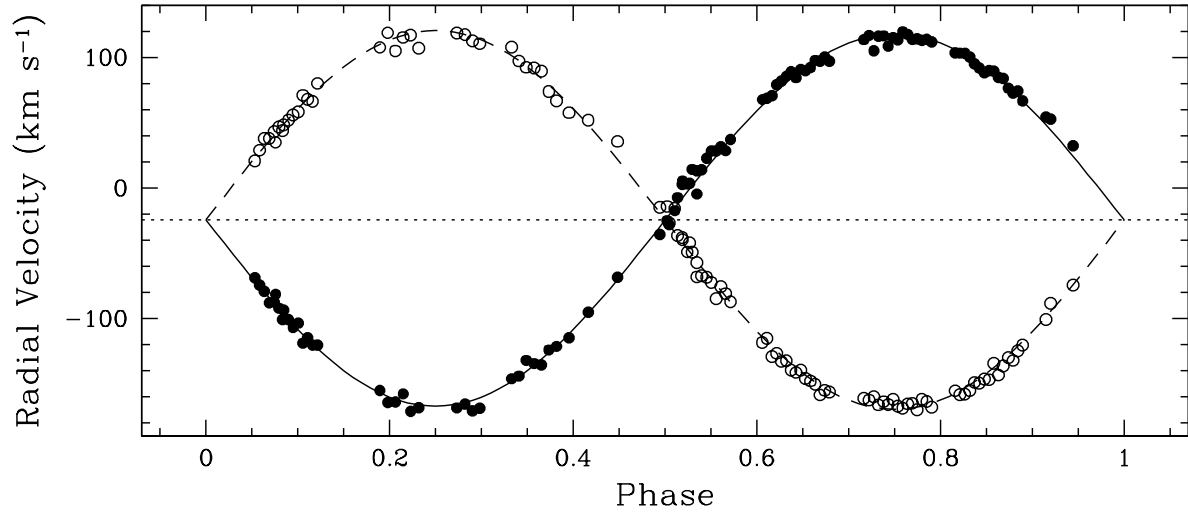


Fig. 2.— Radial velocity curve of GU Boo. The filled and open circles correspond to the velocities of the primary and the secondary, respectively. The solid lines represent the orbital solution obtained with TODCOR, and the dashed line is the velocity of the center of mass of the system.

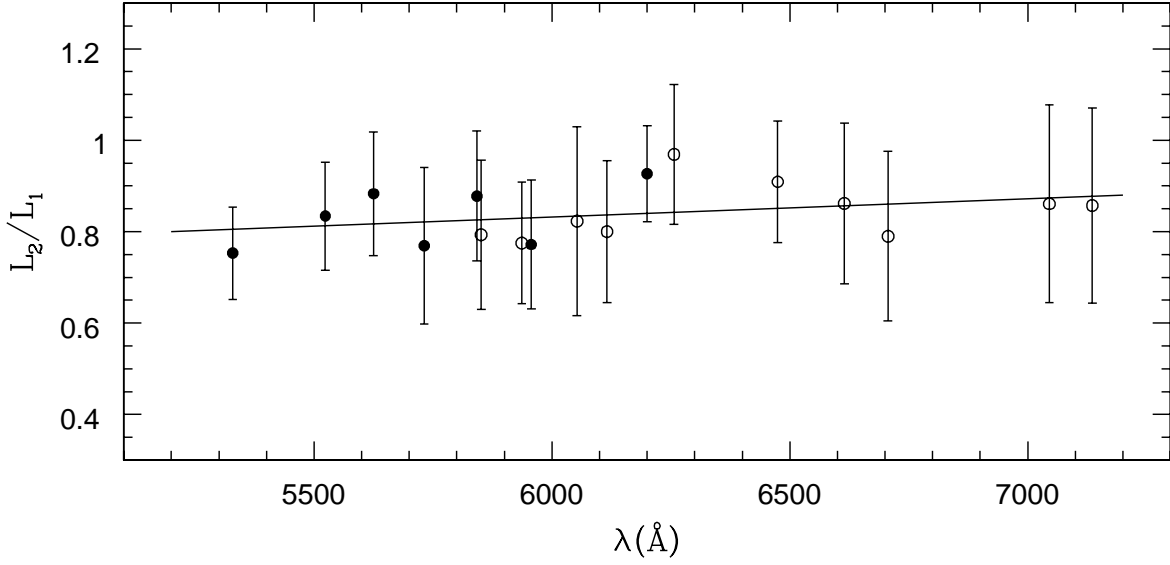


Fig. 3.— Light ratio of the components of GU Boo estimated by TODCOR as a function of wavelength. The filled and open circles correspond, respectively, to the spectra collected on the first and second night of observations. The continuous line represents the best linear fit to the data. Based on that fit, we have adopted an average luminosity ratio for the binary of $L_2/L_1 \simeq 0.84 \pm 0.04$ (at 6200\AA).

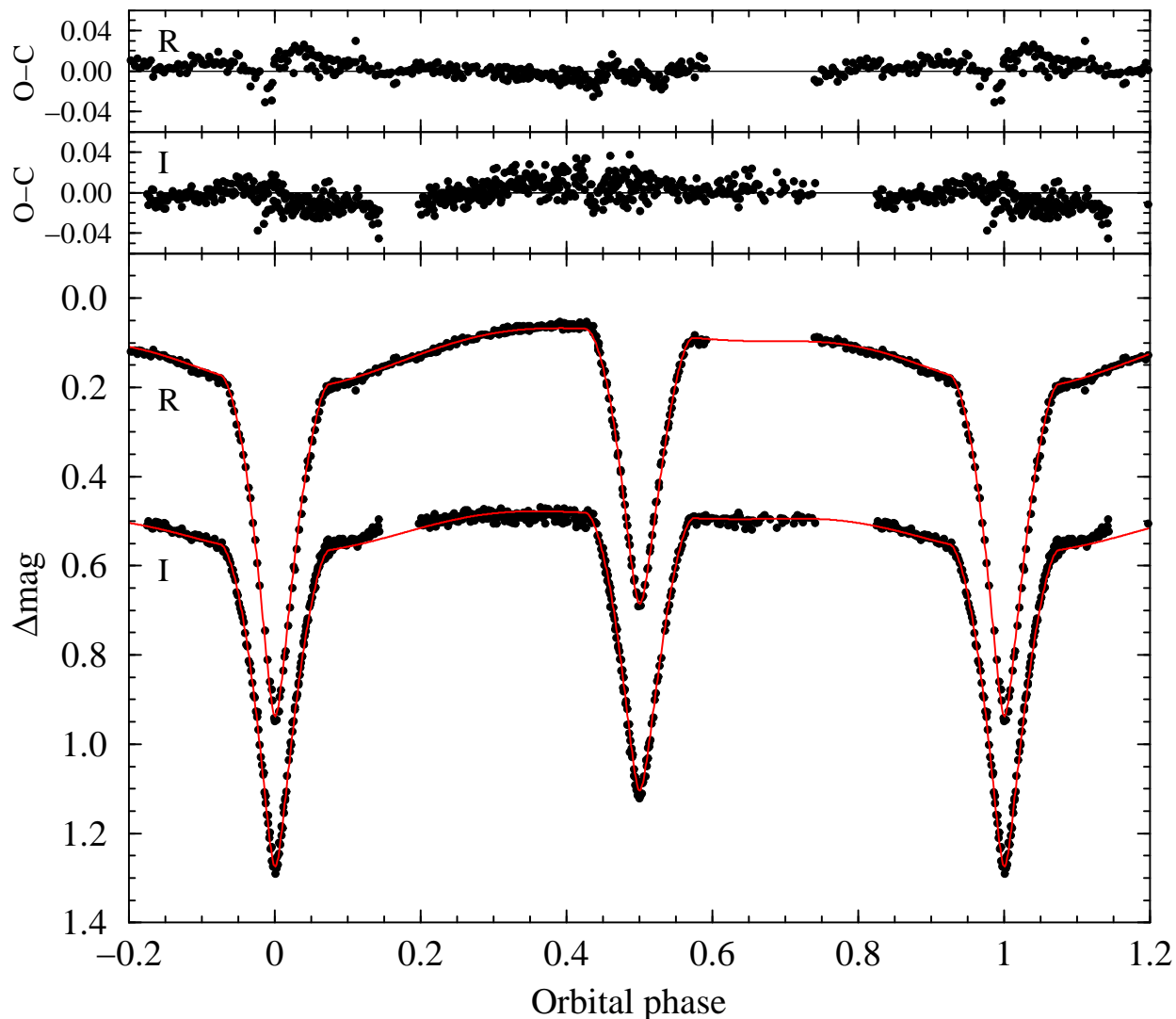


Fig. 4.— R- and I-band light curves of GU Boo collected at the SARA 0.9-m telescope in KPNO, between March 24 and May 6 2003. The dots represent individual observations in each passband, and the continuous lines correspond to the best fits to those light curves using WD2003 (see §4.3 for a detailed discussion of the fitting process). The two diagrams on the top show the residuals of those fits. The average values of the residuals are 0.0086 mag in R and 0.0118 mag in I, respectively.

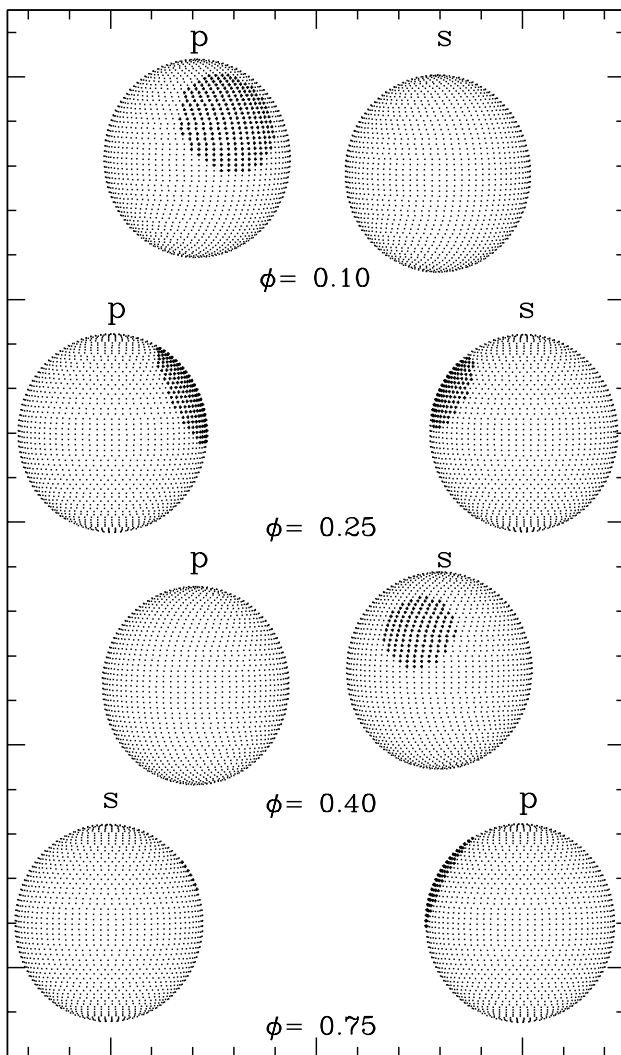


Fig. 5.— Representation of the spot configuration of GU Boo at various orbital phases. The primary and secondary stars are labelled as p and s , respectively. The spot on the primary is cooler than the photosphere, with a temperature factor of $T_{sp}/T_{ph} = 0.94$. The spot on the secondary is a “bright spot” (hotter than the photosphere), with $T_{sp}/T_{ph} = 1.06$. See Table 8 for a summary of the parameters of the spots.

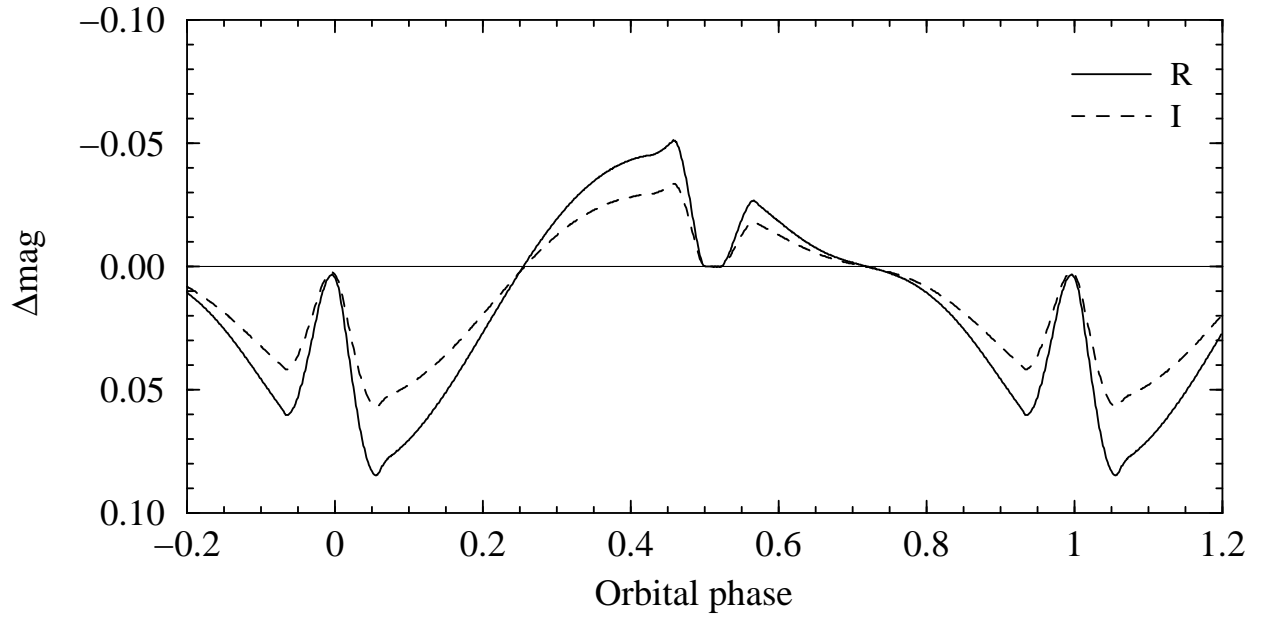


Fig. 6.— Photometric effect of the spots on the light curves. The continuum and dashed lines correspond, respectively, to the R- and I-band curves.

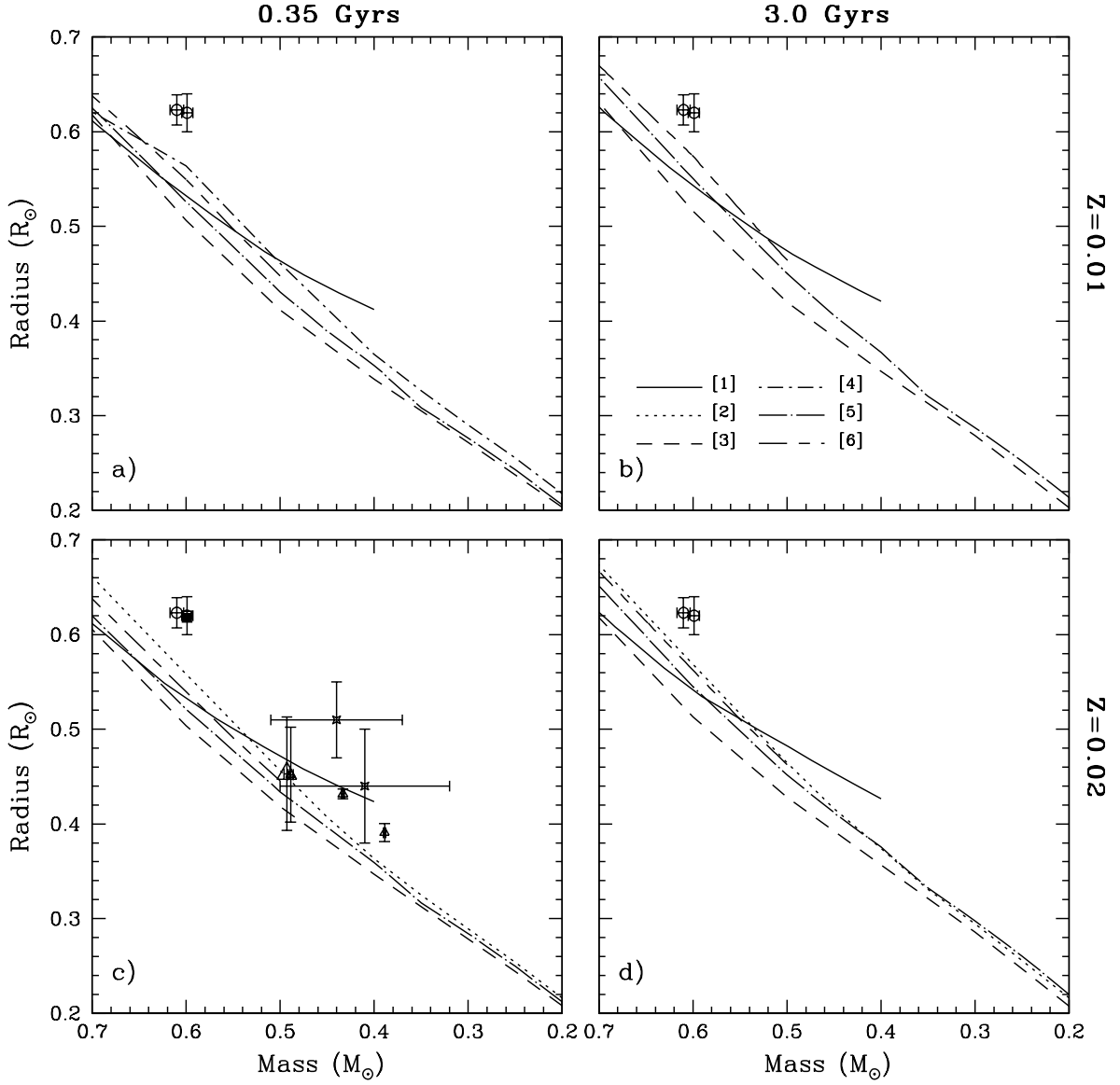


Fig. 7.— Mass-radius relations of stars between 0.7 and 0.2 M_{\odot} predicted by the models in Table 11. Each column corresponds to a different isochrone age (0.35 Gyr on the left, and 3.0 Gyr on the right), while each row represents a different metallicity ($Z = 0.01$ at the top, and $Z = 0.02$ at the bottom). Each trace corresponds to a different model, with the labels [1],[2], [3], ... in diagram b) matching the labels in column 1 of Table 11. The open circles show the location of the stars in GU Boo. In diagram c), the filled circle (overlapping with the less massive component of GU Boo), open triangles, and crosses mark, respectively, the location of the components of YY Gem, CU Cnc, and BW3 V38. The components of the recently found TrES-Her0-07621 are shown as open triangles.

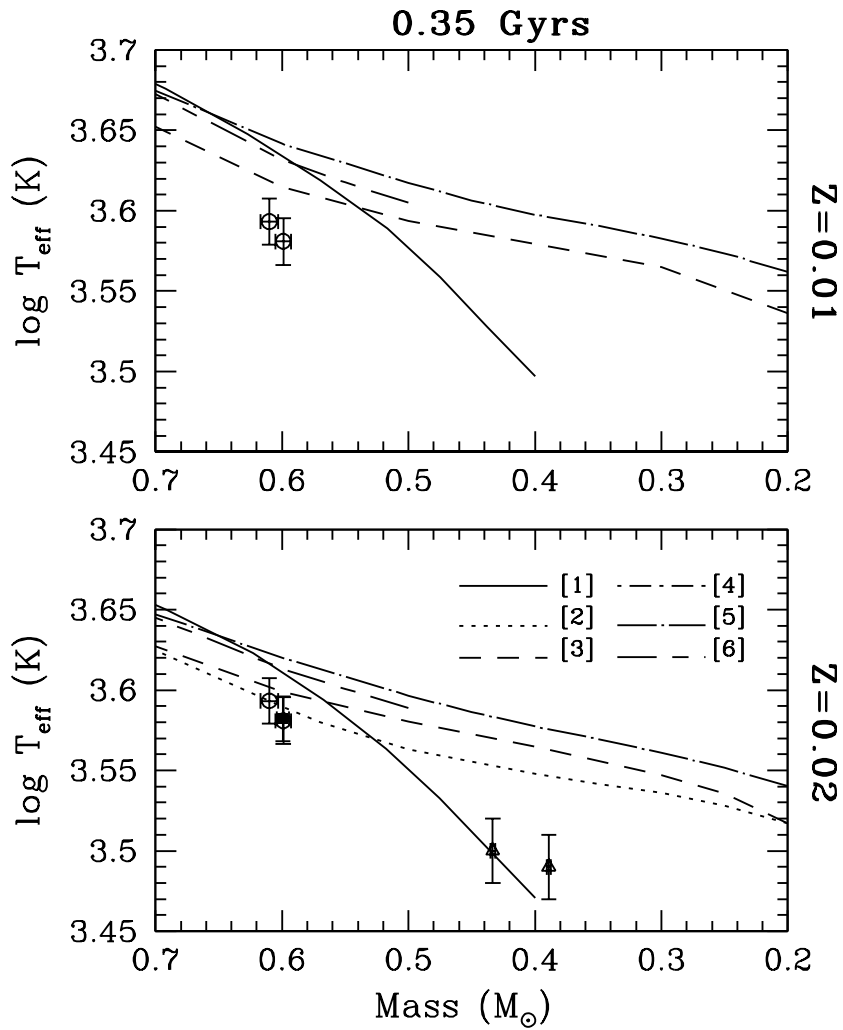


Fig. 8.— Mass- $\log T_{\text{eff}}$ relations of stars between 0.7 and $0.2 M_{\odot}$ predicted by the models in Table 11, for an isochrone age of 0.35 Gyr. The metallicity in each diagram is $Z=0.01$ (top), and $Z=0.02$ (bottom). Each trace represents a different model, following the same convention as in Figure 7. The open circles in each diagram represent the location of the

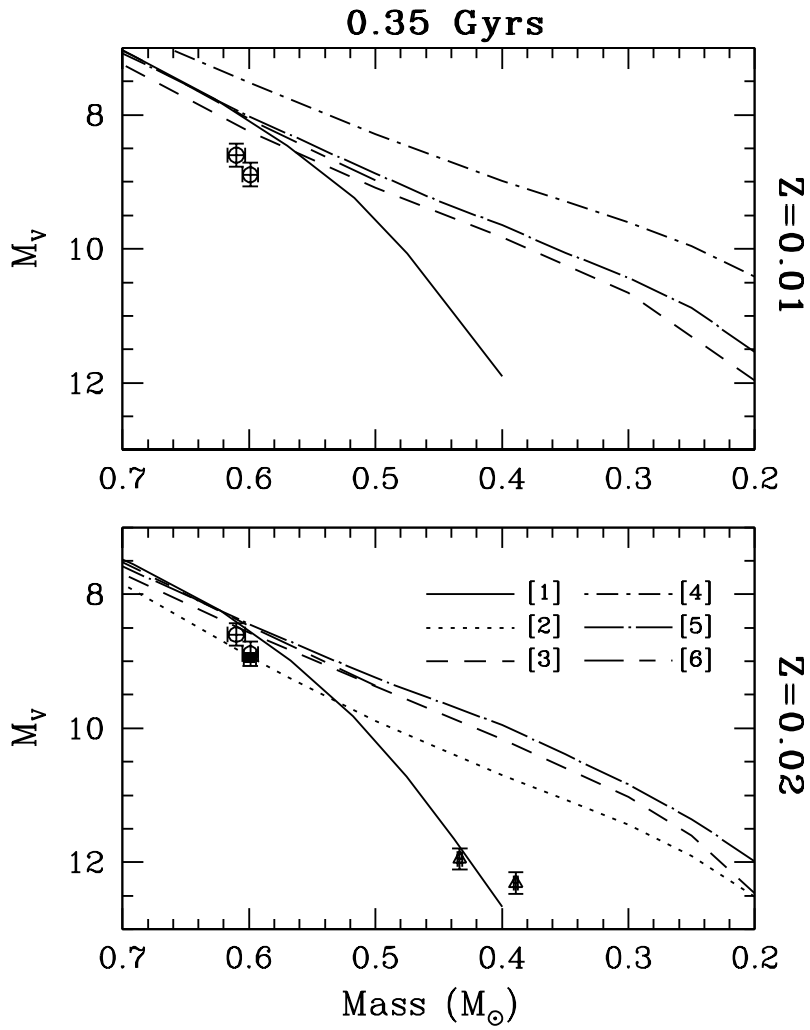


Fig. 9.— Mass- M_V relations of stars between 0.7 and 0.2 M_{\odot} predicted by the models in Table 11, for an isochrone age of 0.35 Gyr. See caption to Fig. 8 for a full description of the plots.

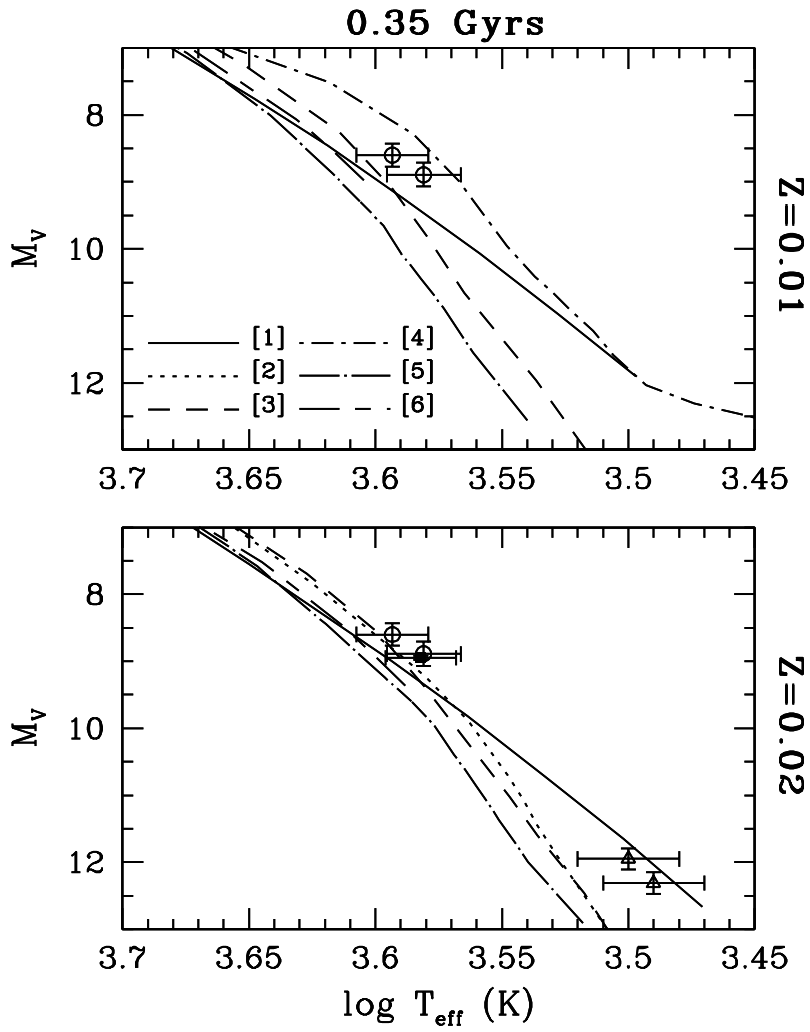


Fig. 10.— $\log T_{\text{eff}}-M_V$ relations of stars between 0.7 and $0.2 M_{\odot}$ predicted by the models in Table 11, for an isochrone age of 0.35 Gyr. See caption to Fig. 8 for a full description of the plots.